



Molecular weight cut off (MWCO) determination in ultra- and nanofiltration: Review of methods and implications on organic matter removal

A. Imbrogno^a, José I. Calvo^b, M. Breida^a, R. Schwaiger^{c,d}, Andrea I. Schäfer^{a,*}

^a Institute for Advanced Membrane Technology (IAMT), Karlsruhe Institute of Technology (KIT), Hermann-von-Helmholtz-Platz 1, 76344 Eggenstein-Leopoldshafen, Germany

^b Surfaces and Porous Materials Group (SMAP), Institute of Sustainable Processes (ISP), Universidad de Valladolid, Dr. Mergelina s/n, 47071 Valladolid, Spain

^c Institute of Energy and Climate Research (IEK), Structure and Function of Materials (IEK-2), Forschungszentrum Jülich, Wilhelm-Johnen-Strasse 52428 Jülich, Germany

^d Karlsruhe Nano Micro Facility (KNMF), Karlsruhe Institute of Technology (KIT), Hermann-von-Helmholtz-Platz 1, 76344 Eggenstein-Leopoldshafen, Germany

ARTICLE INFO

Keywords:

Polyethylene glycol
Oligosaccharide
Pore size distribution
Liquid chromatography
Size exclusion

ABSTRACT

Estimation of membrane molecular weight cut off (MWCO) in the range between ultrafiltration (UF) and nanofiltration (NF) is challenging because retention is not controlled only by size exclusion. This review provides an experimental and theoretical overview of the membrane MWCO in the range from UF to loose NF (from 500 to 0.7 kDa) to evaluate the significance of membrane MWCO on predicting retention of organic solutes when approaching NF pore structure. The experimental section includes filtration of: i) organic tracers with different molecular weights (MW) and properties, such as polyethylene glycol (PEG) and oligosaccharides, and ii) natural organic matter (e.g. humic acid, alginic acid, Tanzanian and Australian organic matter) in the MWCO range between UF and NF, at minimal concentration polarization. The role of molecule structure, size exclusion and charge shielding when filtering organic solutes is elucidated. The molecular structure of uncharged organic tracers plays a major role on MWCO estimation, especially for loose NF membranes, where oligosaccharides are retained more effectively compared to PEG tracers of similar MW. The MWCO determined by PEG filtration and estimated from the pore radius distribution are consistent in the UF range from 1 to 500 kDa, indicating major contribution of size exclusion. Conversely, MWCO of loose NF membranes determined with PEG tracers is overestimated. Charged organics, such as humic acid (1.5 kDa < MW < 3 kDa), shows retention between 60 and 80 % for UF membrane MWCO below 30 kDa (pore radius < 14 nm) and full retention by loose NF (pore radius below 1.4 nm). This is explained with an interplay of size exclusion and charge shielding in the pore. This review can assist in the selection of the organic tracer and operating conditions for membrane MWCO determination between UF and NF, elucidating the relevance of membrane MWCO in organic matter retention.

1. Introduction

Membrane molecular weight cut-off (MWCO) is defined as the MW of the organic tracer that is 90 % retained by the membrane, determined by drawing the organic tracer retention as a function of the tracer MW [1]. An overview of membrane MWCO ranging from nanofiltration/reverse osmosis (NF/RO) to microfiltration (MF), and the corresponding pore diameter is shown in Fig. 1A. A typical range of MWCO for UF membranes is 1–500 kDa [2], while NF membranes typically have a MWCO below 1 kDa (0.15–0.3 kDa) [3]. ‘Loose’ NF membranes have a MWCO

of 0.5–2 kDa with unique properties, including high retention of charged organics (e.g. dyes and organic matter), low salt retention (both monovalent and multivalent), and lower operating pressure than NF (<6 bar) [4–6]. MWCO is a size exclusion parameter that averages the pore size and does not consider molecular interactions (such as adsorption, charge interaction, solute–solvent interaction), which become relevant for separation in the range between UF and NF processes [7–9].

In the following sections, the most commonly applied methods to determine the MWCO of UF and NF membranes are described and the specific limitations are highlighted. These methods are: i) filtration of

* Corresponding author.

E-mail address: Andrea.Iris.Schaefer@kit.edu (A.I. Schäfer).

<https://doi.org/10.1016/j.seppur.2024.128612>

Received 11 June 2024; Accepted 27 June 2024

Available online 3 July 2024

1383-5866/© 2024 The Author(s). Published by Elsevier B.V. This is an open access article under the CC BY license (<http://creativecommons.org/licenses/by/4.0/>).

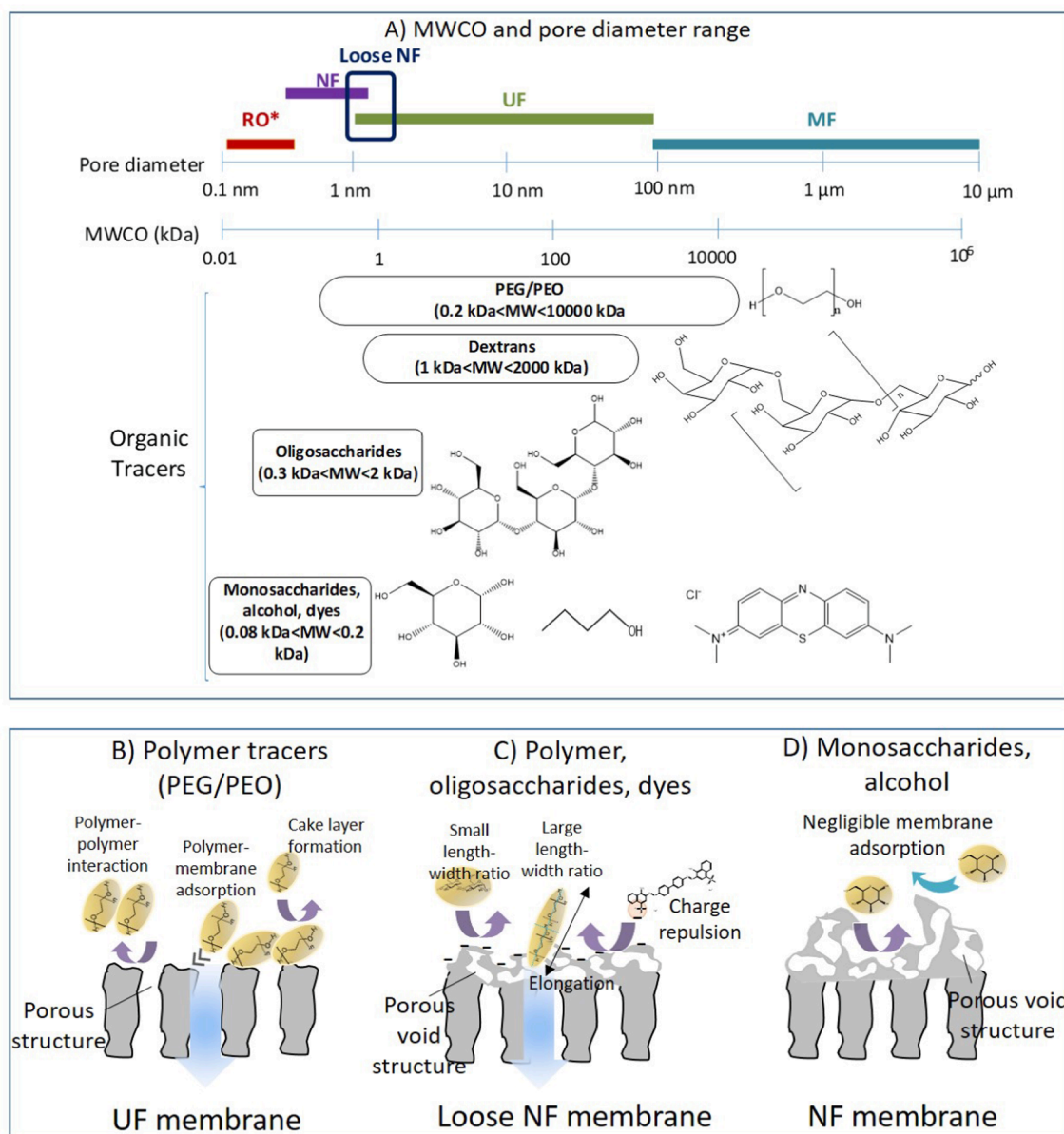


Fig. 1. A) Overview of membrane MWCO, pore diameter, and organic tracers used for MWCO characterization, * pore size for RO membranes refers to void space, B-D) schematics of expected retention and transport mechanisms of different tracers by UF, loose NF and NF membranes. Chemical structures were drawn with ChemDraw Professional.

organic tracers with different MW [10–12], ii) estimation from pore radius distribution by using liquid–liquid displacement porosimetry (LLDP) [13], and iii) coupling of polymer mixture filtration (like PEGs, dextrans) with liquid chromatography [14–17].

Although there is extensive literature available on the UF and NF membrane MWCO characterization with organic tracers, the comparison of studies and results performed with different conditions, devices (hence hydrodynamics), tracers type and a limited range of MWCO is difficult. This is challenging especially at the interface between UF and NF (such as for loose NF), where the MWCO is determined mostly with charged organics, such as dyes [4,6,18–21]. In case of UF membrane MWCO, most of the studies have been performed in a range of tracer concentrations (especially dextran, polyethylene glycols) between 0.3 to 3.6 g/L [11,15,16,22,23] and with tracer mixtures [11,24–26], which enhance concentration polarization leading to artefacts in MWCO determination. For this reason, an extensive experimental section has been included in this review to provide a complete and comprehensive overview of the experimental MWCO determined by filtration of different tracers in the

full range from UF to loose NF membranes (from 500 kDa to 0.7 kDa), under similar filtration, hydrodynamic conditions and minimal concentration polarization. This is relevant to: i) elucidate in which range of MWCO and for which organic tracer type the role of molecular structure and solute-membrane interaction are relevant to control the retention, ii) clarify when the membrane MWCO and solute MW are relevant to predict the retention of natural organics in UF and NF. The experimental section provides a guidance to: i) select the organic tracer type and the operative conditions to estimate the MWCO from the UF to NF range, ii) help in understanding the mechanisms controlling the retention of organic tracer and organic matter from the UF to NF range, and iii) determine the MWCO of loose NF membranes by using oligosaccharides tracers. Experimental results include filtration of different organic tracers (e.g. PEG/PEO and oligosaccharides) as well as organic matter (OM) commonly found in natural water (e.g. humic acid, alginic acid, Tanzanian and Australian OM). This variety of organic solutes and membrane MWCO will lead to a better understanding of which OM and organic tracers are separated based on membrane MWCO.

2. Methods for membrane MWCO determination

2.1. Estimation of UF and NF MWCO from organic tracer filtration

Filtration of organic tracers with different MW is widely applied to estimate MWCO of UF and NF membranes at both laboratory scale and by membrane manufacturers. The most commonly used organic tracers for UF MWCO estimation are neutral polymer tracer solutes, like polyethylene glycol (PEG), polyethylene oxide (PEO), oligostyrene, alkanes, and dextrans (see Fig. 1A) [1,11,12,16,23,27,28]. Various factors can affect the MWCO estimation with this method as the retention of these molecules is not solely controlled by size exclusion. A schematic representation of the retention and transport mechanisms occurring during filtration of organic tracers from UF to NF range is shown in Fig. 1B-D. The transport of smaller MW tracers when present in a mixture with larger MW is hindered by polymer-membrane interaction or pore blockage, solute-solute interactions and cake layer formation by larger MW tracers [11,24–26]. These interactions can result in the creation of MWCO artefacts as the retention is not dominated by size exclusion (see Fig. 1B) [16,23,29]. Additionally, the operating conditions applied in filtration (pressure, polymer concentration and use of mixtures that are not always specified) affect polymer retention due to concentration polarization, usually resulting in underestimation of the MWCO [16,24–26,30].

In the case of NF membranes, saccharides (including mono and disaccharides) and oligosaccharides are used as alternatives to PEG/PEO for MWCO and pore radius estimation because they are neutral and hydrophilic organic molecules with low MW (below 2 kDa) and negligible solute-membrane interaction (see Fig. 1D) [31–33]. When these tracers are used, the presence of defects, defined as non-uniform and highly permeable membrane areas, can interfere with the organic tracer retention based on size exclusion, thus affecting MWCO estimation [34–36].

When approaching the range between UF and NF membranes MWCO, such as the loose NF, the organic tracer molecular shape, size and flexibility become relevant for the separation of low MW organics by size exclusion (see Fig. 1C) [9,37–39]. Molecular shape of organic molecules is usually described by the molecule length and width, and their ratio. Molecule length (L) is defined as the longest distance between two atoms in the molecule when it is projected on a plane with a z - x - y axis. Width and depth are measured by projecting the molecule on the plane perpendicular to the length axis and measuring the longest (width) and shortest (depth) distances (Fig. S1) [37,38,40]. Previous studies reported a sharper increase of organic tracer retention (hence MWCO) by NF when the molecular width is considered instead of MW, because molecules with shorter width can permeate more easily [37,38,41]. This highlights that when approaching the nanoscale pore structure, such as in the UF/NF range, MW cannot predict molecule retention.

Several studies demonstrated that molecular shape plays an important role in controlling not only the molecule size, but also the spatial orientation at the pore entrance [9,20,37,40,42]. Long-chain organics (such as polymer tracers) are subjected to macromolecule deformation (like elongation) under applied pressure, which facilitates permeation especially through NF membranes (see Fig. 1C) [39,43,44]. In fact, polymers with a high length-width ratio (like PEG/PEO or dextran) can elongate more easily than short chain oligomers (like oligosaccharides) or saccharides (with a length-width ratio close to 1), resulting in artefacts for MWCO estimation [9,40,42–45].

Organic tracers with small molecular width and a capsule shaped geometry (like oligosaccharides) are reported to give better prediction of retention (hence MWCO) by NF membranes because retention is controlled by size exclusion [9,37,45,46].

Besides the uncharged organic tracers, charged organic molecules (like natural organic matter, water soluble dyes and polyelectrolytes) have been used for MWCO characterization of NF membranes, especially

for loose NF. However, in this case charge interaction results in a tracer specific MWCO rather than MWCO as an intrinsic membrane property [4,6,18–20,47]. This is because of a synergistic contribution of charge repulsion by the negatively charged NF membranes and size exclusion (Fig. 1C), which is relevant especially for charged low MW dyes [21]. In addition to charge repulsion, the electric double layer within the charged NF membrane pore structure (namely Debye length) can play a role in the retention by size exclusion of electrolytes and charged organics, like natural organic matter (OM), as it changes the actual pore radius of the membrane in the presence of ionic strength [48].

2.2. Estimation of MWCO from liquid-liquid displacement porosimetry (LLDP)

LLDP has been proposed as an alternative method to estimate UF membrane MWCO using the measured pore radius distribution, as opposed to the time-consuming method of organic tracer filtration [13,49]. Other liquid displacing techniques (e.g. mercury porosimetry, bubble point method, thermo and permporometry) [50–52] and the filtration of rigid nanoparticles [53–57] have been used to estimate the pore size distribution of UF membranes. Among the liquid displacing techniques, LLDP is more advantageous as the membrane sample is not destroyed by the high pressure applied and the remaining mercury in the pore structure [58,59]. LLDP is based on the convective transport of a displacing liquid inside the porous membrane (previously wetted by an immiscible liquid). The method uses Young-Laplace equation to describe the pressure difference across the interface of two immiscible liquids assuming a simplified structure of capillary cylindrical pores, to relate the applied pressure and the pore radius opened to flux [59,60]. The resulting flow as a function of pressure (or equivalently, pore radius) is related to the pore radius by the Hagen-Poiseuille equation, which is used to determine the number of pores for each pore radius involved in the flow [59–61]. By applying a pressure gradient, the number of pores involved in the flow increases, resulting in a pore radius distribution as a function of flow [59,60]. Once the normal distribution of the membrane pore radius is obtained, the mean pore radius is used to estimate the size (and accordingly the MW) of the tracer molecules which are expected to be 90 % retained. The use of two immiscible liquids (a wetting and a displacing liquid) in LLDP allows for lower pressure to be applied compared to gas LDP. LLDP allows to measure pore radius below 20 nm with a detection limit approaching 2 nm (dependent on the operating conditions), which is not suitable for NF membranes with pore radius below 1 nm and a porous void structure [58,59,62].

2.3. Estimation of MWCO from mixed organic tracers and liquid separation chromatography

Liquid chromatography (LC) analysis coupled with polymer tracer filtration has been proposed as an alternative method for the estimation of MWCO, when a mixture of polymer tracers with different MW is used [14–16]. This allows to determine the MWCO by performing one filtration, instead of several filtrations of individual polymer tracers. The LC techniques mostly used to identify the polymer tracers permeating through the membrane are: i) high pressure liquid chromatography (HPLC) [14,15], ii) size exclusion chromatography (SEC) or gel permeation chromatography (GPC) [16,17], and iii) LC combined with an organic carbon detector (LC-OCD) in cases of organic solutes separations based on their MW [63,64]. HPLC analysis is limited to a range of PEG MW from 0.7 to 6 kDa, which is suitable for UF with MWCO below 5 kDa and NF membranes [14,15]. Conversely, SEC analysis allows to cover broader UF MWCO due to the possible separation of bigger MW tracers up to 1000 kDa [16]. When separating OM of different MW, LC can be combined with fluorescence, organic carbon detection (OCD) and organic nitrogen detection (OND) [63,64]. LC-OCD is mostly applied to separate OM into biopolymers (BP, MW < 10 kDa), humic substances (HS, MW 1 to 7 kDa), building blocks (BB, MW < 1 kDa), low molecular

weight acids and neutral organics (LMW, MW < 0.4 kDa) [63,64]. The major drawbacks of LC for polymer tracers or OM separation are organic solutes-column interaction and solute-solute interaction, which can result in underestimation of membrane MWCO or artefacts with OM separation and MW determination [17].

2.4. Implication of UF and NF MWCO for organic matter removal

Similar to the filtration of organic tracers for MWCO estimation, the OM retention by UF and NF membranes is controlled by an interplay of different mechanisms, such as size exclusion, charge repulsion, and other solute-membrane interactions. The different mechanisms lead to inconsistent retention of OM based solely on membrane MWCO [65–69]. This is highlighted in several studies where variable range of retention and mechanisms are reported for OM separation by UF and NF membranes.

Humic acid removal from 70 to 86 % has been reported for UF MWCO below 10 kDa, while removal higher than 95 % has been reported for NF with MW of 300 Da [68,70–72]. This was attributed to an interplay of hydrophobic interactions with the membrane and charge repulsion. In contrast, neutral low MW organics (MW 200–400 Da) are less removed by NF with a retention between 80 and 88 % [68,70–72]. Schäfer *et al.* [73] demonstrated that retention of natural organics ranges between 50 and 80 % depending on their MW. The same study reported a sharp increase in retention with membrane pore diameters below 6 nm (MWCO below 10 kDa), due to a dominance of size exclusion. Yu *et al.* [74] reported an inconsistent removal of OM with MW below 0.8 kDa by loose NF membranes (MWCO of 0.8 and 1 kDa), which was pH dependent. This can be attributed to the molecular shape of humic substances containing charged functional groups (e.g. COOH and OH groups), which vary their molecular size under different water conditions (pH and ionic strength) and consequently their retention by size exclusion [48,69].

3. Experimental methodology

3.1. Organic tracer type and solution chemistry

Two polymer tracers were used for MWCO determination, PEG (MW 0.2–35 kDa, purity not specified, Sigma Aldrich, Germany) was used for loose NF and UF MWCO below 30 kDa, and PEO (MW 100–4000 kDa,

purity not specified, Sigma Aldrich, Germany) was used for UF MWCO above 100 kDa. Oligosaccharides (maltose, malto-triose, malto-hexaose, xylo-pentaose and fructo-oligosaccharide from Merck, purity > 90 %, Germany) were selected for MWCO determination of loose NF membranes. Molecule structure and characteristics (pKa, MW, molecular weight, length and Stokes radius) of PEG/PEO and oligosaccharide tracers are reported in Table S1. An individual polymer tracer solution of 0.020 g/L, 0.025 g/L for maltose and 0.023 g/L for the other oligosaccharides (corresponding to 10 mgC/L) was used to minimise concentration polarization according to mass transfer calculations [75]. All solutions were prepared in MilliQ water to avoid interference of ionic strength by the presence of salts for MWCO determination. The resulting pH of the organic tracer solutions prepared in MilliQ water was 5.3 ± 0.4 . To estimate the MWCO from the mean pore radius determined with LLDP, the PEG/PEO tracer water diffusivity (D_w , m^2/sec) was calculated from the tracer MW (g/mol) using Eq. (1), valid in a range of polymer MW between 21 and 530 kDa [13,76].

$$\log D_w = -4.11 - 0.48 \log(MW) \quad (1)$$

3.2. Organic matter type and solution chemistry

Sodium alginate salt (AA, 72 – 78 % purity, Alfa Aesar, Germany) and humic acid (HA, technical grade 80 % purity, Sigma Aldrich, Germany) were used as representative cases of biopolymers and humic substances. Natural waters from Tanzania (Tanz, from a swamp of the Maji ya Chai River [77]) and Australia (Aus, from Gosford Mooney pump station in Brisbane Water National Park, Australia [78]) were used as examples of natural OM. The HA stock solution of 500 mgC/L was prepared by dissolving 0.5 g of powder in 500 mL of MilliQ water, adding 1 g of NaOH and stirring for 24 h. The HA and natural water stock solutions were filtered with a nitrate cellulose 0.45 μm filter to remove suspended solids, and the dissolved organic carbon (DOC) concentration was measured with a total organic carbon analyser (TOC, Sievers M9, General Electric, USA). The OM feed solutions were prepared by diluting a certain volume of the OM stock solutions in a background electrolyte solution containing 1 mM $NaHCO_3$ (99.7 % purity, Bernd Kraft, Germany) and 10 mM NaCl (99.7 % purity, VWR Chemicals, Germany) to have an OM feed concentration of 10 mgC/L. The feed solution pH was adjusted to 8 ± 0.2 by adding HCL 1 M and NaOH 1 M.

Table 1

Nominal MWCO, pore radius, pure water permeability (L_p , L/m^2hbar) and material of Biomax, Ultracel UF and loose NF membranes.

Membrane type	Supplier Code	Nominal MWCO (kDa) ^a	Pore radius (nm) ^b	Top dense layer material	L_p (L/m^2hbar)
Ultracel UF	PLCHK	100	9.1	Regenerated cellulose	200
	PLCTK	30	4.8		130
	PLCGC	10	2.7		80
	PLCCC	5	1.8		10
	PLCBC	3	1.4		5
	PLHAC	1	0.8		4
Biomax UF	PBVK	500	21.3	Polyethersulfone	1330
	PBMK	300	16.2		1620
	PBHK	100	9.1		930
	PBQK	50	6.1		630
	PBTK	30	4.8		503
	PBGC	10	2.6		390
	PBCC	5	1.8		68
Hydracore NF	Hy70	0.7	0.7	Sulfonated polyethersulfone	2.5
	Hy50	1	0.8		14
	Hy10	3	1.4		30

^a Determined by manufacturer at 90 % retention of: i) maltodextrin (for UF MWCO range 1–10 kDa) and dextran mixture (for UF MWCO range 10–1000 kDa) from 0.7 to 3.6 g/L for Biomax and Ultracel [16], 2) dyes (type not specified) retention for Hydracore NF as provided by the supplier [6].

^b Calculated from the MWCO as the equivalent sphere radius $r_p = 2.0374 \cdot 10^{-11} MW^{0.53}$ where r_p (m) is the membrane pore radius [79].

3.3. UF and loose NF membranes characteristics

3.3.1. Membrane MWCO, permeability and pore radius

Biomax and Ultracel UF membranes (Millipore, Bedford, USA) were selected to cover the full range of UF membrane MWCO (1–500 kDa) and representative materials, namely polyethersulfone (Biomax) and regenerated cellulose (Ultracel). Three NF membranes (Nitto-Hydranautics, Germany), namely Hydracore10 (Hy10), Hydracore50 (Hy50) and Hydracore (Hy70), made of sulfonated polyethersulfone were used. These NF membranes have a nominal MWCO that is in the range between UF and NF from 0.7 to 3 kDa. Membrane characteristics (nominal MWCO, pore radius, top dense layer material and pure water permeability) are reported in Table 1.

3.3.2. Membrane surface and cross-section morphology

Microscopy analysis of the membrane surface and cross-section was performed to evaluate the pores spatial distribution and superficial pore structure of membranes with varying MWCO range from UF to NF. Biomax and Ultracel UF membranes were analysed using a helium ion microscope (HIM, ORION NanoFab, Carl Zeiss AG, Germany) at an acceleration voltage of 30 kV and beam current of 0.3 pA. UF membrane samples were soaked for 1 h in MilliQ water and then rinsed to remove the glycerine coating. The membrane coupons were air-dried before analysis with the microscope and no metal sputtering was required. Microscopy imaging of Ultracel membranes was challenging due to the low conductivity of the regenerated cellulose, which could not be solved with metal sputtering. The imaging of Ultracel membranes with MWCO below 100 kDa was not successful. Hydracore NF membrane surface and cross-section were imaged with a scanning electron microscope (Ultra 55 SEM, Carl Zeiss Ltd., Germany) at the Leibniz Institute of Surface Engineering (IOM), with sample preparation and analysis conditions for the NF membranes reported elsewhere [80]. Images are shown in Fig. 2.

A highly porous surface is evident for Biomax membranes with a

larger MWCO (300–500 kDa) and heterogeneous pore entrance structure. For membranes with MWCO below 300 kDa the superficial pores are less visible and the membrane surface becomes denser. When approaching UF and loose NF membrane MWCO below 5 kDa, the membrane surface appears dense without visible superficial pores.

3.3.3. Membrane surface charge and Debye length

Ultracel and Biomax UF membranes, as well as Hydracore NF membranes are negatively charged at pH above 2 [80–82]. At pH 8, corresponding to the pH at which OM filtration was performed, zeta potentials values (determined with streaming potential measurements) reported in previous studies are in the range of –10 to –19 mV for Ultracel and Biomax [81,82], and –30 mV for Hydracore NF membranes [80]. Given the negative charge of the membranes and the presence of an electrolyte background of 10 mM NaCl and 1 mM NaHCO₃ in the feed solution containing OM, the Debye length within the porous structure of UF and NF membranes was calculated. The aim was to determine the contribution of charge shielding by the electric double layer of the ions in the pore to OM retention. The Debye length, λ_D (m) was calculated using Eq. (2) [83,84]:

$$\lambda_D = \left(\frac{\varepsilon_0 \varepsilon_r RT}{F^2 \sum_i z_i^2 c_i} \right)^{1/2} \quad (2)$$

where ε_0 is the permittivity of vacuum ($8.85 \cdot 10^{-12}$ C/V.m), ε_r is the relative permittivity (78.2), R is the gas constant (8.3143 J/mol.K), T is the temperature (K), F is Faraday's constant (96487 C/mol), z_i is the valence of ion i (1 for NaCl and NaHCO₃), and c_i is the ion concentration (11 mol/m³). A Debye length of 4.1 nm for loose NF membranes with pore radius in the range 0.7 to 1.4 nm (see Table 1) and an electrolyte background of 10 mM NaCl and 1 mM NaHCO₃ was calculated, which is similar to the value reported by Boussouga *et al.* [84] (~3.0 nm) for NF membranes (NF270, NF90) and similar electrolyte background of 10 mM NaCl. The Debye ratio (or feed screening length) (λ) is obtained by

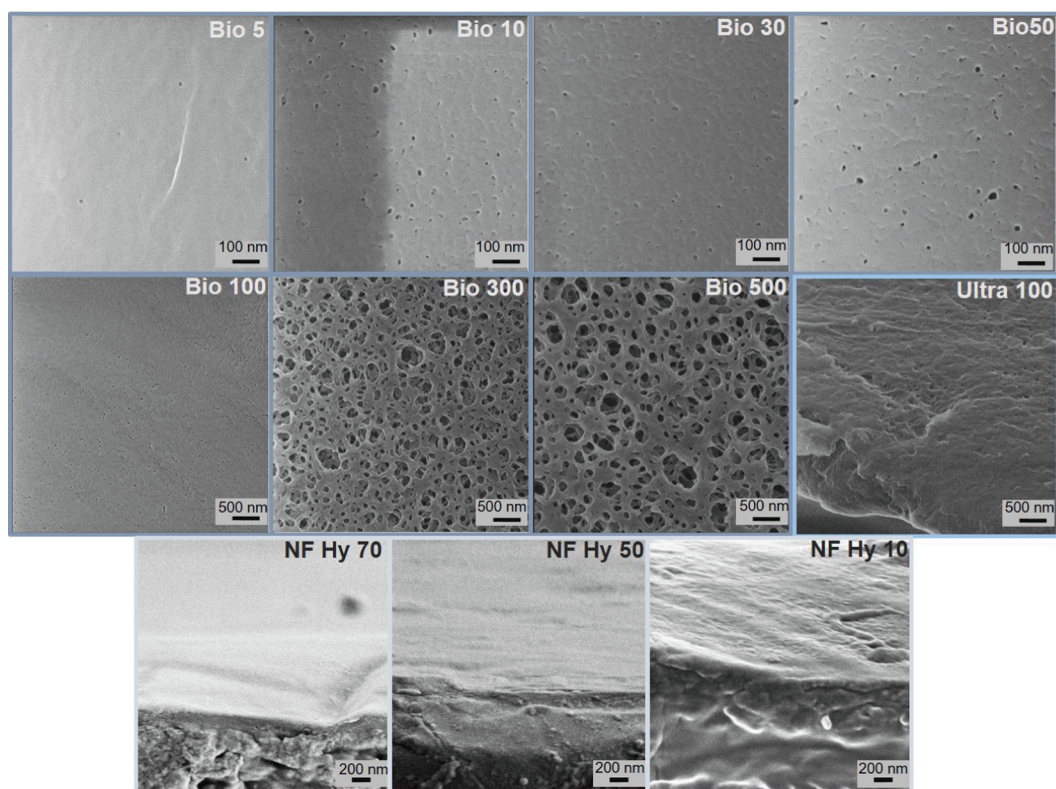


Fig. 2. HIM micrographs of Biomax (Bio) and Ultracel (Ultra) UF membrane surface (resolution 100 nm for MWCO from 5 to 50 kDa, 500 nm resolution for MWCO from 100 to 500 kDa). SEM micrographs of NF Hydracore (NF Hy) are adapted from Boussouga *et al.* [80]

dividing the Debye length by the membrane pore radius (r_p) as presented in Eq. (3). This parameter is relevant to determine the variation of charge shielding within the pore when the pore radius (hence the MWCO) is varied [83].

$$\lambda = \frac{\lambda_D}{r_p} \quad (3)$$

3.4. Filtration equipment and protocol

A stainless steel dead-end stirred cell was used for: i) organic tracer filtration of different MW to determine the retention and membrane MWCO of UF and loose NF, and ii) OM filtration through UF membranes with a range of MWCO between 1 and 50 kDa and loose NF to evaluate the role of membrane MWCO on the separation of different OM. A detailed description of the filtration protocol is given in Table S2. Some of the operating conditions (recovery of 30 %, stirring speed 400 rpm, and feed concentration of 10 mgC/L) were similar to the MWCO characterization protocol for NF membranes reported previously [75]. The range of fluxes, pressures and temperatures are reported in Table S3. PEG/PEO filtration by UF membranes was performed at a fixed permeate flow rate of 0.35 ± 0.04 L/h for membranes with MWCO ranging from 5 to 500 kDa and 0.17 L/h for Ultracel membranes with MWCO ranging from 1 to 3 kDa. The permeate flow rate was controlled with a flow regulator valve (SS-2MG Swagelok, Germany) installed in the permeate side (system schematic is depicted in Fig. S2). For loose NF membranes, PEG/PEO filtration was performed at a flux of 20 L/m²h due to the limited permeability of Hy70 and the highest possible pressure achievable in the system (9.6 bar). Observed retention (R_{obs}), determined experimentally from the feed and permeate concentration at 15 % recovery, was used for the MWCO estimation with PEG/PEO and oligosaccharides at minimal concentration polarization as previously reported [75].

3.5. Pore size distribution by liquid–liquid displacement porosimetry (LLDP)

An automated liquid–liquid displacement porosimetry (LLDP), built at the University of Valladolid, was used to measure the pore radius distribution of Biomax and Ultracel UF membranes in the range of MWCO from 1 to 500 kDa to estimate the MWCO from the pore radius distribution [85]. NF pore radius distribution was not measured by LLDP due to pressure limitations and a pore radius detection limit of 2 nm [59,60]. Biomax membranes were soaked for 1 h in MilliQ water to remove glycerine and freeze-dried (Alpha 2–4 LSC plus, Germany) for 22 h at a temperature of -20 °C and a pressure of 0.0001 mbar prior to analysis. Ultracel membranes were not freeze dried because shrinkage of

the membrane at similar conditions was observed afterwards. The flow of the displacing liquid was controlled by a syringe pump, the pressure was monitored by a pressure transducer (0–5 MPa, DFP®, AEP), the membrane holder area was $2.5 \cdot 10^{-4}$ m² and the analysis was performed at a controlled temperature of 20 ± 0.1 °C. The membrane coupon was soaked for 45 min in wetting liquid containing isobutanol saturated with water (1/1, v/v) prior to LLDP analysis. The displacing liquid was water saturated with isobutanol (1/1, v/v) and pumped through the membrane coupon at a pressure ranging between 0.1 and 40 bar.

The log-normal distribution function was used to obtain the differential permeability distribution as a function of the mean membrane pore radius and the normal pore radius distribution versus permeability [86]. MWCO was estimated from the mean pore radius following the method published by Calvo *et al.* [13] In this method, the pore radius (r_p , m) that covers 90 % of the cumulative pore radius distribution was converted to MWCO by considering the equivalent spherical radius of the PEG/PEO tracer molecule and the PEG/PEO tracer water diffusivity. The assumptions to apply this method for MWCO estimation are: i) neutral spherical organic tracer, ii) negligible tracer-membrane interaction, iii) retention by size exclusion, and iv) molecule flexibility or deformation at the pore entrance is negligible. Assumption (ii) is valid as negligible PEG/PEO adsorption by UF Biomax and Ultracel membranes was observed, while assumptions (i) and (iv) simplify the real conditions, where PEG/PEO tracer may elongate (high length- width ratio) under applied pressure in filtration (hence no spherical shape) [20,37,40,42].

3.6. Organic matter fractionation by LC-OCD analysis

LC-OCD (Model 9, DOC Labor, Germany) was used to determine the OM type and MW in the feed, retentate and permeate samples after filtration by UF and NF membranes. A SEC column (Toyopearl HW50-S, Tosoh Bioscience, Japan) was used for the separation of OM based on the different elution times when the solution was pumped at a constant flow rate of 2 mL/min (Azura P 4.1S, Knauer, Germany). ChromLOG and ChromCALC software (version 2.5) were used for organic carbon and UV signal processing and data acquisition. A TOC calibration was performed with standard solutions of potassium hydrogen phthalate (purity > 99.5 %, Merck, Germany) in a concentration between 0.1 and 5 mgC/L. The calibration and the limit of detection are reported in Fig. S5B. To relate the MW of OM with the elution time, the system was calibrated using standard molecules of different MW ranging from 0.2 to 65 kDa. The standards type and MW are given in Table S4 and the calibration is shown in Fig. S5. The standard solutions were prepared at 5 mgC/L in MilliQ water and the pH was adjusted to 8.0 ± 0.5 . A dilution factor of two and five was used for OM permeate and feed samples, respectively, before LC-OCD analysis to have a DOC concentration below 5 mgC/L.

Table 2
Organic matter type in the feed, MW, hydrodynamic radius (r_h).

OM	Fractions by LC-OCD	MW from LC-OCD (kDa) ^d	MW range (kDa)	r_h (nm)
AA	BIO: 96 %	65	12–180 [88]	–
HA	HS: 37 %	1.5–2.7	0.2–30 [89,90] ^a	0.3–1.5 [91,92] ^b
	BB: 20 %	1		
	LMW: 31 %	Acids < 0.5 Neutral 0.2		
Aus	HS: 67 %	HS:1.5–2.7	0.5–1.5 [64] ^c	–
	BB: 13 %	BB:1		
	LMW: 20 %	LMW: Acids < 0.5		
Tanz	HS: 75 %	Neutral 0.2	0.5–1.5 [64] ^c	–
	BB: 15 %			
	LMW: 10 %			

^a determined by GPC of HA natural sources.

^b measured by FFF and FFF combined with UF fractionation.

^c determined by LC-OCD,^d determined from the elution time and calibration in Fig. S4 and Fig. S5, BIO = biopolymers, HS = humic substances, LMW = low molecular weight neutrals and acids, BB = building blocks, from Nguyen *et al.* [93].

OM types contained in the feed are given in Table 2. Aus and Tanz waters have a higher HS content compared to HA. HS are negatively charged at pH above 4 due to the deprotonation of COOH groups present in humic acid and fulvic acid ($pK_a = 4.3$) [87], hence charge repulsion by UF and NF membranes is expected.

3.7. Total organic carbon analysis

The concentration of PEG/PEO, oligosaccharides and OM in feed, retentate and permeate samples was measured using a total organic carbon (TOC) analyser (Sievers M9, General Electric, USA). The analysis was performed using an acid and oxidizer flow rate of 1 $\mu\text{L}/\text{min}$. A dilution factor of two was used for the feed, retentate and permeate samples to have a TOC below 10 mgC/L . A calibration with standard solutions of potassium hydrogen phthalate (purity > 99.5 %, Merck, Germany) in a range of concentrations from 0.1 to 10 mgC/L was performed, see Fig. S3.

4. Experimental overview of organic tracer and organic matter retention

Membrane MWCO of UF and NF was determined experimentally by PEG/PEO and oligosaccharide filtration at the point of 90 % retention. The role of molecular structure (short chain oligosaccharides versus long-chain polymer tracers) and adsorption on tracer retention and, consequently, MWCO determination were elucidated. Furthermore, the removal of different OM types commonly found in natural waters and the OM MW not retained by the membranes were determined to elucidate the contribution of size exclusion in the range between UF and NF.

4.1. UF membrane MWCO by PEG/PEO tracer retention

Tracer retention of PEG/PEO of different MW was investigated to evaluate the consistency between tracer MW and UF membrane MWCO at 90 % retention in the range between 1 and 500 kDa (Fig. 3).

For UF Biomax membranes (Fig. 3A and B) with a nominal MWCO between 5 and 100 kDa, the experimental MWCO was determined when the observed retention reached 90 % for PEG/PEO MW of 4, 8, 20 and 100 kDa, respectively. In the case of Ultracel membranes (Fig. 3C and D)

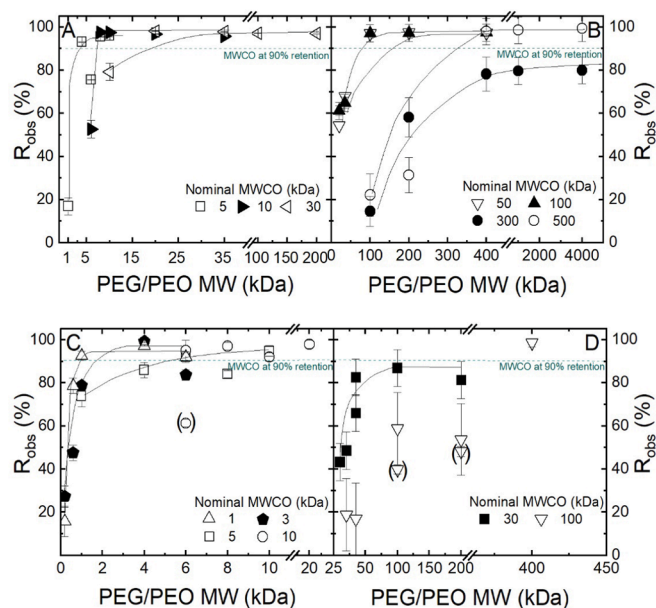


Fig. 3. PEG/PEO observed retention by (A, B) Biomax and (C, D) Ultracel UF membranes (10 mgC/L PEG/PEO in MilliQ, 15 % recovery, 400 rpm, pH 5.3 \pm 0.4, 23.2 \pm 1.3 $^{\circ}\text{C}$). Data points in brackets are repeated experiments.

with a nominal MWCO between 1 and 30 kDa, the experimental MWCO was obtained when the observed retention reached 90 % for PEG MW of 1, 4, 6, 8 and 35 kDa, consistently with the nominal MWCO.

An overestimation of the experimental MWCO was observed for the UF membranes with nominal MWCO of 100 kDa (Fig. 3D), where the observed retention reached 90 % with PEG MW above 400 kDa. Similarly, for the nominal MWCO of 500 kDa (Fig. 3B), the observed retention reached 90 % with PEG MW above 400 kDa, while it remained to 80 % for 300 kDa, considering the experimental error. One explanation for the overestimated MWCO could be the occurrence of PEO interaction with the membrane [11], resulting in higher retention. Loss of up to 25 % of the PEO mass in the feed (Fig. S12) and a flux reduction after filtration between 50 and 85 % (Fig. S13) were observed, which could be related to the occurrence of PEO deposition in the membrane for larger MWCO. While PEO deposition in the membrane could be more relevant for larger UF membrane MWCO, polymer adsorption was negligible for UF MWCO below 100 kDa, displaying no interference with the UF MWCO estimation. In the next step, the role of tracer molecular structure on loose NF MWCO estimation was investigated.

4.2. Loose NF membrane MWCO by PEG/PEO and oligosaccharide tracer retention

PEG/PEO (long-polymer chain) and oligosaccharide (spherical colloid structure) retention by loose NF membranes was investigated to determine if the molecular structure of uncharged tracer interferes with the MWCO estimation. The observed retention as a function of tracer MW is shown in Fig. 4.

When oligosaccharide tracers (spherical colloid structure) were filtered, 90 % retention was reached with xylo-pentaose (0.7 kDa) for Hy70 and fructo-oligosaccharide (1.9 kDa) for Hy50, indicating a MWCO of 0.7 and 2 kDa, respectively. Surprisingly, PEG tracers (long-polymer chains) with similar MW to oligosaccharides showed lower retention (below 20 %), and the 90 % retention was reached with PEG MW of 35 kDa, resulting in an unrealistic MWCO for loose NF membranes.

Possible reasons for such a variable MWCO with different tracers could be: i) tracer adsorption on the membrane, and ii) the molecular structure associated with different molecule size. PEG mass loss at the low feed concentration of 10 mgC/L was negligible within the experimental error (Fig. S15), suggesting that PEG adsorption on the membrane was not responsible for the different MWCO. In terms of molecular structure, PEG tracers are long polymer chains with a molecule length about 1.6 times (for MW below 1.5 kDa) larger than the

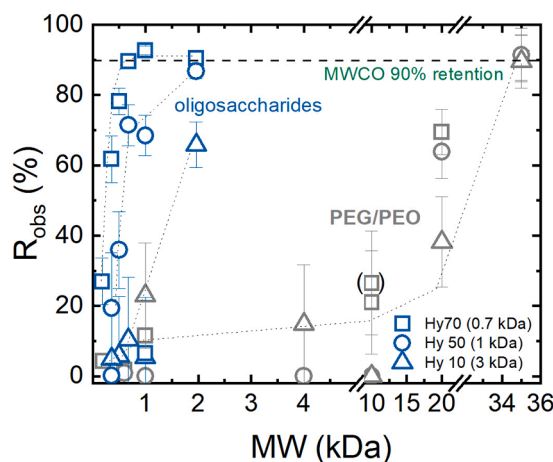


Fig. 4. PEG/PEO and oligosaccharide retention by loose NF membranes Hy70, Hy50 and Hy10 (10 mgC/L in MilliQ, 21.4 \pm 2.6 $\text{L}/\text{m}^2\text{h}$, stirrer speed 400 rpm, 24 \pm 2 $^{\circ}\text{C}$, 15 % recovery, pH 5.3 \pm 0.4).

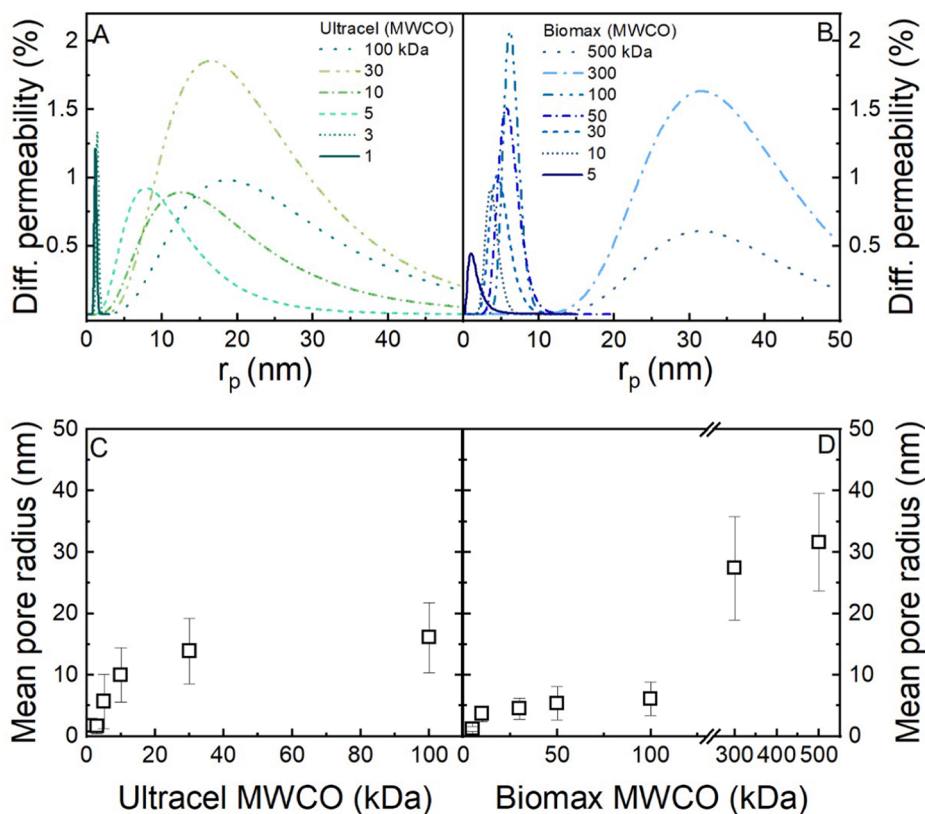


Fig. 5. Log-normal differential permeability distribution of Ultracel (A) and Biomax (B) membranes as a function of mean pore radius determined by LLDP, (C-D) mean pore radius extrapolated from the permeability distribution as a function of membrane MWCO. Error bars are standard deviation of the pore radius measurements from the permeability distribution.

oligosaccharides, and a molecule width about 3.6 times smaller (Table S1). Hence, PEG tracers could more easily elongate at the pore entrance and permeate through the porous structure compared to the oligosaccharides with a more spherical colloid structure. Similar findings were reported by Liu *et al.* [42], who demonstrated that the long polymer shape of PEG tracers (larger length/width ratio) facilitates elongation at the pore entrance and permeation by NF, resulting in lower retention of PEG molecules compared to oligosaccharides.

4.3. Size exclusion in organic tracer retention by UF and NF

The role of size exclusion in MWCO estimation with PEG/PEO tracers was determined from the pore radius distribution obtained with LLDP.

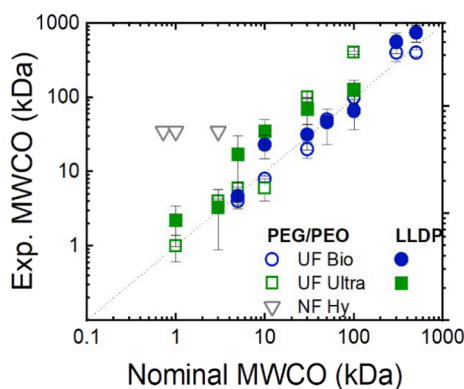


Fig. 6. Log-normal plot of experimental and nominal MWCO determined with PEG/PEO filtration for UF and loose NF and calculated from LLDP for UF (10 mgC/L, MilliQ, 15 % recovery, 101 ± 5 L/m²h for Biomax, 35 ± 5 L/m²h for Ultracel 1–3 kDa, pH 5.3 ± 0.4 , 22.8 ± 1.2 °C).

The normalized pore radius distribution as well as the mean pore radius of UF Biomax and Ultracel membranes are reported in Fig. 5A–D.

Mean pore radius increased from 2 to 32 nm with the increase of UF membrane MWCO ranging from 1 to 500 kDa (Fig. 5 C,D). This is consistent with the range of pore radius reported in literature for UF membranes (between 2 and 24 nm) [61,86,94].

A wider pore radius distribution was observed for UF membranes with larger MWCO above 100 kDa (Fig. 5A and B), which can be explained with the standard deviation of the normal distribution being proportional to the mean pore radius. The wider distribution indicates more variability in porous structure and size for larger UF membrane MWCO (consistent with the heterogeneous porous structure of HIM images in Fig. 2). This can result in less predictable MWCO estimation from the retention of organic tracers with different MW.

The contribution of size exclusion was elucidated by comparing the MWCO estimated from the pore radius measured by LLDP, with the experimental MWCO determined by PEG/PEO tracer filtration. The log-normal distribution of experimental MWCO and the MWCO estimated from the pore radius is shown in Fig. 6. The MWCO determined experimentally by PEG/PEO filtration was similar to the MWCO estimated from LLDP for the UF membranes. This is an indication that PEG/PEO retention is mostly controlled by size exclusion and that polymer MW is an appropriate size exclusion parameter for UF membranes. This result was expected since PEG/PEO tracers are uncharged molecules (pK_a ~ 16–18, see Table S1) and the experimental MWCO was determined at low tracer concentration (in MilliQ water), which provided negligible concentration polarization and tracer adsorption onto the membrane. Similar results were reported in previous studies by Calvo *et al.* [13,49], who compared the experimental MWCO of UF membranes determined with dextran tracers and the MWCO estimated from LLDP.

In the case of loose NF membranes, the MWCO determined experimentally by PEG filtration was clearly overestimated compared to the

nominal MWCO (0.7 to 3 kDa). This discrepancy suggests that polymer MW is not an appropriate size exclusion parameter when approaching loose NF MWCO. Notably, a comparison between the PEG tracer chain width (0.3 to 0.32 nm, see Table S1) and the nominal pore radius estimated from MWCO (0.7 to 1.4 nm, see Table 1) revealed that the PEG width is 2 to 5 times smaller than the pore radius. This indicates that retention is predominantly controlled by the width of the polymer chain when approaching loose NF MWCO.

4.4. Size exclusion in OM retention by UF and NF

Previous results obtained with organic tracers suggested that molecular structure is a relevant size exclusion parameter, especially in the range between UF and NF. The role of size exclusion under varying membrane MWCO was further investigated to separate different OM types, commonly present in natural waters. Observed retention and permeate concentrations of different OM filtered with different membrane MWCO are shown in Fig. 7.

The results presented in Fig. 7 indicate that alginic acid (AA) was retained above 90 % by loose NF and UF membranes, irrespective of membrane MWCO. This was expected given the larger MW of AA with 65 kDa (see Table 2) compared to the membrane MWCO up to 50 kDa.

In contrast, humic acid (HA) and OM of natural waters from Australia (Aus) and Tanzania (Tanz) were highly retained (above 80 %) by loose NF and UF with MWCO below 3 kDa. This observation is consistent with the range of HA MW reported in Table 2 (MW of 1.5 to 2.7 kDa), as well as the retention reported in literature for UF membranes with MWCO below 10 kDa (up to 70 %) and NF membranes (up to 90 %) [68,70–73]. For larger UF membrane with MWCO above 10 kDa, HA would be expected to be poorly retained due to the lower MW. However, a retention in the range between 36 and 80 % was observed for UF MWCO above 10 kDa. Similarly, when natural waters (Aus and Tanz) were filtered, retention remained constant at about 40 % for a UF MWCO > 10 kDa.

These results indicated that OM type strongly affected the retention by UF with different membrane MWCO, and that there was not a clear correlation between the OM type and the membrane MWCO. Given the heterogeneous composition of natural waters, the different OM MW present in the permeate were analyzed to relate the OM MW with the membrane MWCO and to elucidate the contribution of size exclusion. The various OM types in the permeate and feed samples reported as humic substances (HS), building blocks (BB), and low molecular weight acids and neutrals (LMW) separated with UF and NF membranes are shown in Fig. 8 and Fig. S4, respectively.

When HA was filtered (Fig. 8 A and E), low MW neutrals and acids (200 to 400 Da, Table 2) were the dominant OM type in the permeate of UF membranes below 3 kDa and loose NF membranes (Fig. S4), which is plausible given the smaller MW compared to the membrane MWCO range. A similar result was observed for natural water OM (Aus and Tanz) (Fig. 8 B, D, F, H), where HS and low MW acids were the dominant OM types in the permeates filtered with UF MWCO above 3 kDa.

A different OM composition of the permeate was observed when HA was filtered with larger UF MWCO. Notably, the HS peak did not appear at UF MWCO below 30 kDa (Fig. 8 A and E), which indicated that HS was fully retained despite the larger pore radius (below 14 nm) compared to the HS hydrodynamic radius range (0.3–1.5 nm) and MW (1.5 to 2.7 kDa). This result suggested that HA retention was not controlled solely by size exclusion as there is not a clear correlation between HS retention and the membrane MWCO. HS is known to have functional groups, such as COOH groups, that can deprotonate at pH above 4 ($pK_a \sim 4$) providing negative charge which may result in: i) charge repulsion by the negatively charged membrane, and ii) charge shielding by the electric double layer in the porous structure [48,68,69].

4.5. Charge shielding on OM retention in the range between UF and NF

In presence of ionic strength and charged NF membranes, the formation of an electric double layer (Debye length) in the pores occurs

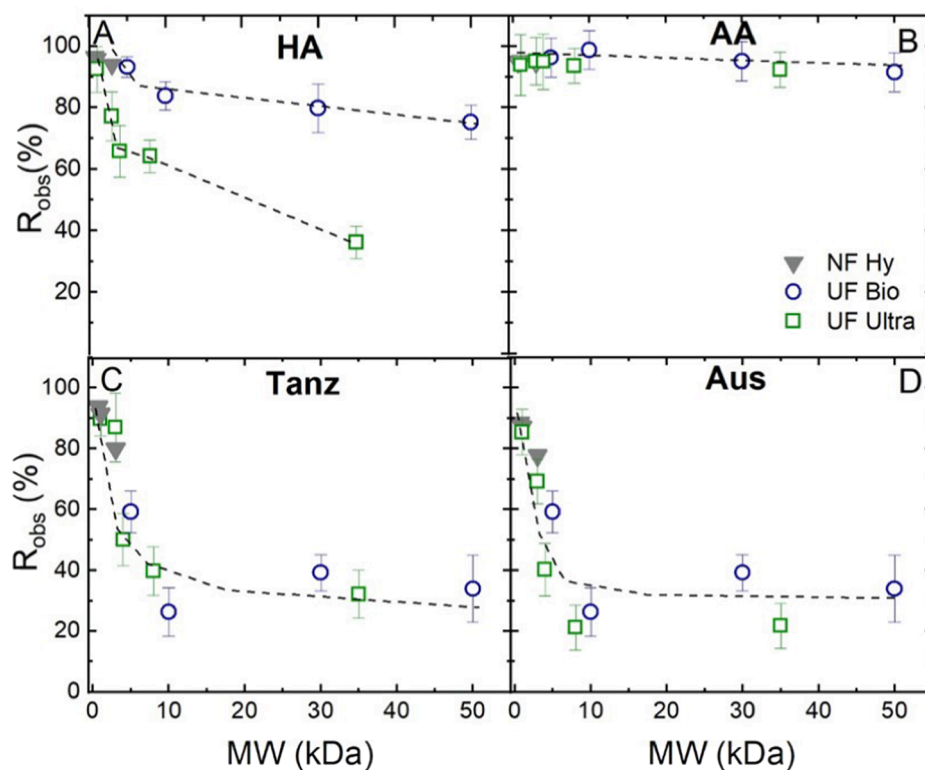


Fig. 7. OM observed retention at different membrane MWCO and organics (10 mgC/L, 1 mM NaHCO₃, 10 mM NaCl, 15 % recovery, 400 rpm, pH 8 ± 0.2, 23.2 ± 1.6 °C). Data for Aus, HA and AA with NF Hydracore are adapted from Gopalakrishnan *et al.* [95].

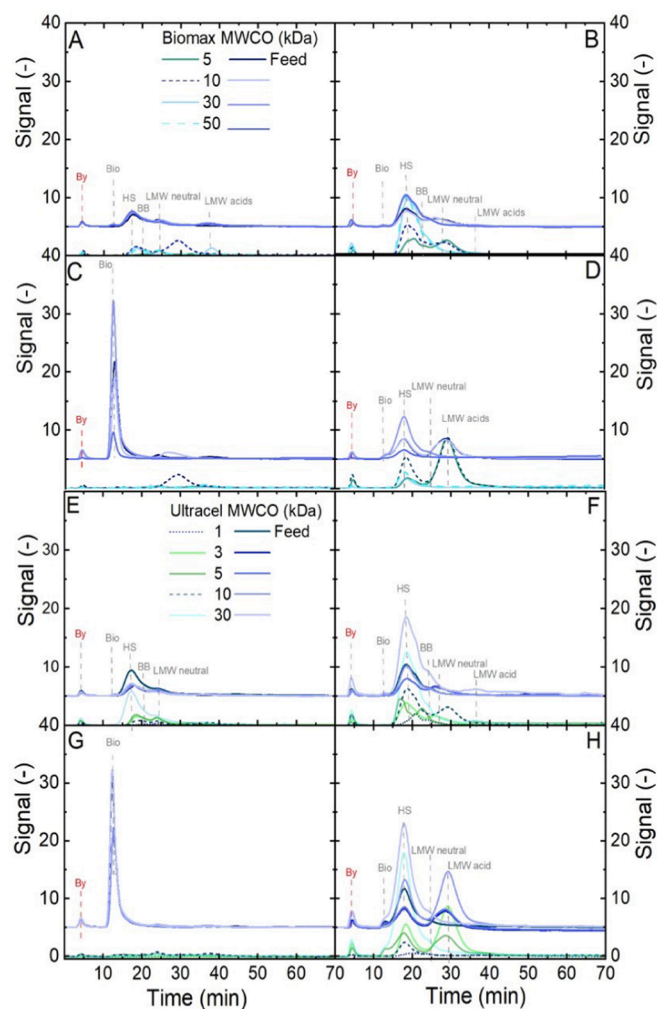


Fig. 8. Organic carbon signal in the feed and permeate samples of (A, E) humic acid, (B, F) Australian OM, (C, G) alginate acid, (D, H) Tanzanian OM filtered by Biomax (A–D) and Ultracel (E–F) (10 mgC/L, 1 mM NaHCO₃, 10 mM NaCl, 15 % recovery, and 400 rpm, pH 8 ± 0.2).

resulting in a charge shielding, which varies the effective pore radius [48]. The variation of the Debye ratio (electric double layer) as a function of membrane pore radius and MWCO was investigated to elucidate the role of charge shielding on the OM retention in the range between UF and NF. The relation is shown in Fig. 9A and schematics of charge shielding within the pores are depicted in Fig. 9B–C.

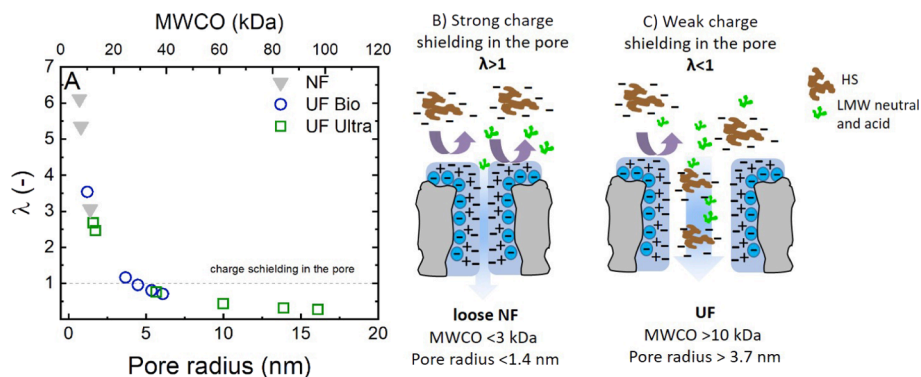


Fig. 9. A) Debye ratio as a function of membrane pore radius and the corresponding MWCO in the range between UF and NF and constant ionic strength (electrolyte background of 10 mM NaCl and 1 mM NaHCO₃), B and C) schematic of Debye screening layer within the pore of a loose NF and UF membrane and its effect on the retention of different OM.

Debye ratio (λ) (Fig. 9A) decreased with the increase of pore radius and membrane MWCO, confirming that the charge shielding in the pore by the electric double layer is more significant for smaller pore radius. This is consistent with literature where it is stated that when the pore radius approaches value smaller than the Debye length (such as in NF), the electric double layer overlaps and charge shielding is stronger [83,96]. At pore radius above 3.7 nm (UF MWCO > 10 kDa), the Debye ratio decreased to values below 1. This indicates that charge shielding in the pore is weaker and consequently the retention of charged OM, such as HS is lower (Fig. 9C). This is consistent with the results of HA and natural OM retention reported in Fig. 7, where HA retention between 35–40 % was observed irrespective of UF MWCO. At pore radius below 3.7 nm (UF MWCO < 10 kDa), λ is larger than 1 indicating a more dominant effect of charge shielding by the electric double layer within the pore. This means that charge shielding becomes stronger at smaller pore radius, enhancing the size exclusion of HA with charge repulsion.

These findings highlight that when approaching loose NF membranes, charge shielding by the electric double layer and size exclusion contribute to the retention of charged OM, such as HA, which cannot be predicted solely by the HA MW and hydrodynamic radius [48,71,72]. In the case of UF membranes with MWCO above 10 kDa, the contribution of charge repulsion is weaker than loose NF due to a weaker electric double layer within the pores.

5. Conclusions

Three main conclusions can be drawn from this review. When uncharged organic tracers are filtered, the molecular structure plays a major role than the MW to explain retention by size exclusion for loose NF. In fact, an inconsistent membrane MWCO was obtained when the MW of the organic tracer was considered, as reported for the loose NF membranes and PEG/PEO tracers. By looking at the molecular structure (chain width and length) of PEG/PEO and oligosaccharides, it was observed that the width of the polymer tracer controlled predominantly the retention by size exclusion. In contrast, for colloidal shape oligosaccharides, the retention as a function of MW was consistent with the MWCO. In the case of UF membranes with MWCO > 5 kDa, the polymer tracer MW is an appropriate size exclusion parameter to predict membrane retention as demonstrated by the similar log-plot of the experimental MWCO and the one calculated from the pore radius measured with LLDP.

In the case of charged organic solutes, such as humic acids commonly found in natural water, the charge interaction and charge shielding by the electric double layer (Debye length) are involved in the retention by loose NF membranes. By increasing the membrane MWCO > 10 kDa, although the charge shielding is less significant, the retention of humic acids is still controlled by an interplay of charge interaction and size exclusion and the electric double layer, which varies the actual pore

diameter. Hence, the retention of OM cannot be predicted by looking solely at the organic solute MW in both cases of UF and loose NF membranes.

In conclusion, at the interface between UF and NF (such as loose NF) the membrane MWCO can be considered a useful parameter to predict the retention of small uncharged organics with colloidal shaped structure (saccharides with MW < 2 kDa), while it is not useful to predict the retention of uncharged organics with high length to width ratio (e.g. long chain polymers) and charged organics (e.g. organic matter). The results reported in this review are useful to predict the retention mechanisms when loose NF membranes are applied for retention of organic micropollutants with various molecular structure and charge properties.

CRedit authorship contribution statement

A. Imbrogno: Writing – original draft, Data validation and Curation, Investigation, Conceptualization. **José I. Calvo:** LLDP Analysis, Methodology. **M. Breida:** OM experiments, Data analysis. **R. Schwaiger:** HIM morphology analysis, Methodology. **Andrea I. Schäfer:** Conceptualization, Funding acquisition, Resources, Writing – review editing, Supervision.

Declaration of competing interest

The authors declare that they have no known competing financial interests or personal relationships that could have appeared to influence the work reported in this paper.

Data availability

Data will be made available on request.

Acknowledgements

Helmholtz Recruitment Initiative and Helmholtz ERC Recognition Award NAMEPORED for IAMT funding. Millipore and Nitto Hydraulics who kindly supplied the membranes. Regional Government of Castilla and León and the EU-FEDER (CL-EI-2021-07, UIC 082) for funding support on LLDP. Nozipho Gumbi, Julia Wolters and Anna Lisa Vocaturo for performing the PEG/PEO filtration experiments with Biomax, Ultracel and Hydracore membranes, respectively. Prof. Mathias Ulbricht is thanked for the useful discussion on oligosaccharides application for MWCO estimation. Dr. Minh Nguyen for performing LC-OCD analysis of OM samples. Stephan Weyand (IAM, KIT) for performing HIM analysis of the membrane samples and Dr. Kristina Fischer (IOM, Leibniz Institute of Surface Engineering) for SEM analysis. Karlsruhe Nano Micro Facility (KNMF) is thanked for provision of access to the HIM microscope.

Appendix A. Supplementary data

Supplementary data to this article can be found online at <https://doi.org/10.1016/j.seppur.2024.128612>.

References

- A.R. Cooper, D.S. Van Derveer, Characterization of ultrafiltration membranes by polymer transport measurements, *Sep. Sci. Technol.* 14 (1979) 551–556.
- D. Mosqueda-Jimenez, R. Narbaitz, T. Matsuura, G. Chowdhury, G. Pleizier, J. Santerre, Influence of processing conditions on the properties of ultrafiltration membranes, *J. Membr. Sci.* 231 (2004) 209–224.
- M. Paul, S.D. Jons, Chemistry and fabrication of polymeric nanofiltration membranes: a review, *Polymer* 103 (2016) 417–456.
- S. Guo, Y. Wan, X. Chen, J. Luo, Loose nanofiltration membrane custom-tailored for resource recovery, *Chem. Eng. J.* 409 (2021) 127376.
- J. Lin, C.Y. Tang, C. Huang, Y.P. Tang, W. Ye, J. Li, J. Shen, R. Van den Broeck, J. Van Impe, A. Volodin, A comprehensive physico-chemical characterization of superhydrophilic loose nanofiltration membranes, *J. Membr. Sci.* 501 (2016) 1–14.
- R. Boda W. Bates C. Bartels Use of color removal membranes on waste water treatment in the pulp and paper industry MDIW, *Membranes in drinking and industrial water treatment 2010 Trondheim, Norway*.
- A. El Fadil, R. Verbeke, M. Kyburz, P.E. Aerts, I.F. Vankelecom, From academia to industry: Success criteria for upscaling nanofiltration membranes for water and solvent applications, *J. Membr. Sci.* 675 (2023) 121393.
- B. Sutariya, S. Karan, A realistic approach for determining the pore size distribution of nanofiltration membranes, *Sep. Purif. Technol.* 293 (2022) 121096.
- R. Verbeke, I. Nulens, M. Thijs, M. Lenaerts, M. Bastin, C. Van Goethem, G. Koeckelberghs, I.F. Vankelecom, Solutes in solvent resistant and solvent tolerant nanofiltration: How molecular interactions impact membrane rejection, *J. Membr. Sci.* 121595 (2023).
- C. Causserand, P. Aimar, Characterization of filtration membranes, in: *Comprehensive Membrane Science and Engineering*, Elsevier, Oxford, 2010, pp. 311–335.
- C. Causserand, S. Rouaix, A. Akbari, P. Aimar, Improvement of a method for the characterization of ultrafiltration membranes by measurements of tracers retention, *J. Membr. Sci.* 238 (2004) 177–190.
- G. Bousou, B. Van der Bruggen, A. Volodin, C. Van Haesendonck, J. Delcour, P. Van der Meer, C. Vandecasteele, Characterization of commercial nanofiltration membranes and comparison with self-made polyethersulfone membranes, *Desalination* 191 (2006) 245–253.
- J.I. Calvo, R.I. Peinador, P. Prádanos, L. Palacio, A. Bottino, G. Capannelli, A. Hernández, Liquid–liquid displacement porosimetry to estimate the molecular weight cut-off of ultrafiltration membranes, *Desalination* 268 (2011) 174–181.
- L. Xu, S. Shahid, J. Shen, E.A.C. Emanuelsson, D.A. Patterson, A wide range and high resolution one-filtration molecular weight cut-off method for aqueous based nanofiltration and ultrafiltration membranes, *J. Membr. Sci.* 525 (2017) 304–311.
- R. Rohani, M. Hyland, D. Patterson, A refined one-filtration method for aqueous based nanofiltration and ultrafiltration membrane molecular weight cut-off determination using polyethylene glycols, *J. Membr. Sci.* 382 (2011) 278–290.
- G. Tkacik, S. Michaels, A rejection profile test for ultrafiltration membranes & devices, *Nat. Bio/Technol.* 9 (1991) 941–946.
- Y. Chung, Y.-J. Kim, J.F. Kim, M.-Y. Lee, S.-E. Nam, S. Kang, Preparation method of standard molecules for the precise estimation of molecular weight cut-off of membranes by gel permeation chromatography, *Desalin. Water Treat.* 180 (2020) 74–79.
- S. Lee, G. Park, G. Amy, S.-K. Hong, S.-H. Moon, D.-H. Lee, J. Cho, Determination of membrane pore size distribution using the fractional rejection of nonionic and charged macromolecules, *J. Membr. Sci.* 201 (2002) 191–201.
- R. Han, S. Zhang, D. Xing, X. Jian, Desalination of dye utilizing copoly (phthalazinone biphenyl ether sulfone) ultrafiltration membrane with low molecular weight cut-off, *J. Membr. Sci.* 358 (2010) 1–6.
- B. Van der Bruggen, J. Schaepe, D. Wilms, C. Vandecasteele, Influence of molecular size, polarity and charge on the retention of organic molecules by nanofiltration, *J. Membr. Sci.* 156 (1999) 29–41.
- M. Hu, S. Yang, X. Liu, R. Tao, Z. Cui, C. Matindi, W. Shi, R. Chu, X. Ma, K. Fang, Selective separation of dye and salt by PES/SPSf tight ultrafiltration membrane: roles of size sieving and charge effect, *Sep. Purif. Technol.* 266 (2021) 118587.
- M. Bakhshayeshi, A. Teella, H. Zhou, C. Olsen, W. Yuan, A.L. Zydney, Development of an optimized dextran retention test for large pore size hollow fiber ultrafiltration membranes, *J. Membr. Sci.* 421 (2012) 32–38.
- C. Causserand, G. Pierre, S. Rapenne, J.-C. Schrotter, P. Sauvade, O. Lorain, Characterization of ultrafiltration membranes by tracer's retention: Comparison of methods sensitivity and reproducibility, *Desalination* 250 (2010) 767–772.
- C.J. Yehli, A.L. Zydney, Characterization of dextran transport and molecular weight cutoff (MWCO) of large pore size hollow fiber ultrafiltration membranes, *J. Membr. Sci.* 119025 (2020).
- S. Mochizuki, A.L. Zydney, Dextran transport through asymmetric ultrafiltration membranes: comparison with hydrodynamic models, *J. Membr. Sci.* 68 (1992) 21–41.
- M. Bakhshayeshi, D.M. Kanani, A. Mehta, R. van Reis, R. Kuriyel, N. Jackson, A. L. Zydney, Dextran sieving test for characterization of virus filtration membranes, *J. Membr. Sci.* 379 (2011) 239–248.
- P. Prádanos, J. Arribas, A. Hernandez, Hydraulic permeability, mass transfer, and retention of PEGs in cross-flow ultrafiltration through a symmetric microporous membrane, *Sep. Sci. Technol.* 27 (1992) 2121–2142.
- G. Trägårdh, Characterization methods for ultrafiltration membranes, *Desalination* 53 (1985) 25–35.
- C. Tam, A. Tremblay, Membrane pore characterization—comparison between single and multicomponent solute probe techniques, *J. Membr. Sci.* 57 (1991) 271–287.
- A.L. Zydney, A. Xenopoulos, Improving dextran tests for ultrafiltration membranes: effect of device format, *J. Membr. Sci.* 291 (2007) 180–190.
- H. Liu, L. Zhao, L. Fan, L. Jiang, Y. Qiu, Q. Xia, J. Zhou, Establishment of a nanofiltration rejection sequence and calculated rejections of available monosaccharides, *Sep. Purif. Technol.* 163 (2016) 319–330.
- J. Otero, O. Mazarrasa, J. Villasante, V. Silva, P. Prádanos, J. Calvo, A. Hernández, Three independent ways to obtain information on pore size distributions of nanofiltration membranes, *J. Membr. Sci.* 309 (2008) 17–27.
- L.D. Nghiem, A.I. Schäfer, M. Elimelech, Removal of natural hormones by nanofiltration membranes: measurement, modeling, and mechanisms, *Environ. Sci. Technol.* 38 (2004) 1888–1896.

- [34] X. Song, B. Gan, S. Qi, H. Guo, C.Y. Tang, Y. Zhou, C. Gao, Intrinsic nanoscale structure of thin film composite polyamide membranes: Connectivity, defects, and structure–property correlation, *Environ. Sci. Technol.* 54 (2020) 3559–3569.
- [35] A. Ben-David, R. Bernstein, Y. Oren, S. Belfer, C. Dosoretz, V. Freger, Facile surface modification of nanofiltration membranes to target the removal of endocrine-disrupting compounds, *J. Membr. Sci.* 357 (2010) 152–159.
- [36] C. Causserand, P. Aïmar, C. Vilani, T. Zambelli, Study of the effects of defects in ultrafiltration membranes on the water flux and the molecular weight cut-off, *Desalination* 149 (2002) 485–491.
- [37] Y. Kiso, K. Muroshige, T. Oguchi, M. Hirose, T. Ohara, T. Shintani, Pore radius estimation based on organic solute molecular shape and effects of pressure on pore radius for a reverse osmosis membrane, *J. Membr. Sci.* 369 (2011) 290–298.
- [38] V. Yangali-Quintanilla, A. Sadmani, M. McConville, M. Kennedy, G. Amy, A QSAR model for predicting rejection of emerging contaminants (pharmaceuticals, endocrine disruptors) by nanofiltration membranes, *Water Res.* 44 (2010) 373–384.
- [39] S. Eder, P. Zueblin, M. Diener, M. Peydayesh, S. Boulos, R. Mezzenga, L. Nyström, Effect of polysaccharide conformation on ultrafiltration separation performance, *Carbohydr. Polym.* 260 (2021) 117830.
- [40] J.L. Santos, P. de Beukelaar, I.F. Vankelecom, S. Velizarov, J.G. Crespo, Effect of solute geometry and orientation on the rejection of uncharged compounds by nanofiltration, *Sep. Purif. Technol.* 50 (2006) 122–131.
- [41] K.O. Agenson, J.-I. Oh, T. Urase, Retention of a wide variety of organic pollutants by different nanofiltration/reverse osmosis membranes: controlling parameters of process, *J. Membr. Sci.* 225 (2003) 91–103.
- [42] Y.-L. Liu, W. Wei, X.-M. Wang, H.-W. Yang, Y.F. Xie, Relating the rejections of oligomeric ethylene glycols and saccharides by nanofiltration: Implication for membrane pore size determination, *Sep. Purif. Technol.* 205 (2018) 151–158.
- [43] H. De Balmann, R. Nobrega, The deformation of dextran molecules. Causes and consequences in ultrafiltration, *J. Membr. Sci.* 40 (1989) 311–327.
- [44] D.R. Latulippe, J.R. Molek, A.L. Zydney, Importance of biopolymer molecular flexibility in ultrafiltration processes, *Ind. Eng. Chem. Res.* 48 (2009) 2395–2403.
- [45] Y. Kiso, K. Muroshige, T. Oguchi, T. Yamada, M. Hirose, T. Ohara, T. Shintani, Effect of molecular shape on rejection of uncharged organic compounds by nanofiltration membranes and on calculated pore radii, *J. Membr. Sci.* 358 (2010) 101–113.
- [46] V.A. Montesdeoca, J. Bakker, R. Boom, A.E. Janssen, A. Van der Padt, Ultrafiltration of non-spherical molecules, *J. Membr. Sci.* 570 (2019) 322–332.
- [47] N. Hilal, M. Al-Abri, H. Al-Hinai, Characterization and retention of UF membranes using PEG, HS and polyelectrolytes, *Desalination* 206 (2007) 568–578.
- [48] A. Braghetta, F.A. DiGiano, W.P. Ball, Nanofiltration of natural organic matter: pH and ionic strength effects, *J. Environ. Eng.* 123 (1997) 628–641.
- [49] J.I. Calvo, R.I. Peinador, V. Thom, T. Schleuss, K. ToVinh, P. Prádanos, A. Hernández, Comparison of pore size distributions from dextran retention tests and liquid-liquid displacement porosimetry, *Microporous Mesoporous Mat.* 250 (2017) 170–176.
- [50] E. Jakobs, W. Koros, Ceramic membrane characterization via the bubble point technique, *J. Membr. Sci.* 124 (1997) 149–159.
- [51] A. Hernandez, J. Calvo, P. Prádanos, F. Tejerina, Pore size distributions of track-etched membranes; comparison of surface and bulk porosities, *Colloids Surf. A Physicochem. Eng. Asp.* 138 (1998) 391–401.
- [52] C. Zhao, X. Zhou, Y. Yue, Determination of pore size and pore size distribution on the surface of hollow-fiber filtration membranes: a review of methods, *Desalination* 129 (2000) 107–123.
- [53] E. Arkhangelsky, A. Duek, V. Gitis, Maximal pore size in UF membranes, *J. Membr. Sci.* 394 (2012) 89–97.
- [54] A. Duek, E. Arkhangelsky, R. Krush, A. Brenner, V. Gitis, New and conventional pore size tests in virus-removing membranes, *Water Res.* 46 (2012) 2505–2514.
- [55] P. Kosiol, B. Hansmann, M. Ulbricht, V. Thom, Determination of pore size distributions of virus filtration membranes using gold nanoparticles and their correlation with virus retention, *J. Membr. Sci.* 533 (2017) 289–301.
- [56] F. Fallahianbijan, S. Giglia, C. Carbelli, A.L. Zydney, Use of fluorescently-labeled nanoparticles to study pore morphology and virus capture in virus filtration membranes, *J. Membr. Sci.* 536 (2017) 52–58.
- [57] Q. Chan, M. Entezarian, J. Zhou, R. Osterloh, Q. Huang, M. Ellefson, B. Mader, Y. Liu, M. Swierczek, Gold nanoparticle mixture retention test with single particle detection: a fast and sensitive probe for functional pore sizes of ultrafiltration membranes, *J. Membr. Sci.* 599 (2020) 117822.
- [58] M.B. Tanis-Kanbur, R.I. Peinador, X. Hu, J.I. Calvo, J.W. Chew, Membrane characterization via evaporimetry (EP) and liquid-liquid displacement porosimetry (LLDP) techniques, *J. Membr. Sci.* 586 (2019) 248–258.
- [59] M.B. Tanis-Kanbur, R.I. Peinador, J.I. Calvo, A. Hernández, J.W. Chew, Porosimetric membrane characterization techniques: a review, *J. Membr. Sci.* 118750 (2020).
- [60] N. Mkhaidze, R. Gotsiridze, S. Mkhaidze, D. Pattyn, Determination of the polymeric membranes pore size distribution by the method of capillary flow porometry, *Bull. Georgian Natl. Acad. Sci.* 14 (2020).
- [61] S. Giglia, D. Bohonak, P. Greenhalgh, A. Leahy, Measurement of pore size distribution and prediction of membrane filter virus retention using liquid-liquid porometry, *J. Membr. Sci.* 476 (2015) 399–409.
- [62] J.I. Calvo, R.I. Peinador, P. Prádanos, A. Bottino, A. Comite, R. Firpo, A. Hernández, Porosimetric characterization of polysulfone ultrafiltration membranes by image analysis and liquid-liquid displacement technique, *Desalination* 357 (2015) 84–92.
- [63] M.-H. Cai, Y.-P. Wu, W.-X. Ji, Y.-Z. Han, Y. Li, J.-C. Wu, C.-D. Shuang, G.V. Korshin, A.-M. Li, W.-T. Li, Characterizing property and treatability of dissolved effluent organic matter using size exclusion chromatography with an array of absorbance, fluorescence, organic nitrogen and organic carbon detectors, *Chemosphere* 243 (2020) 125321.
- [64] S.A. Huber, A. Balz, M. Abert, W. Pronk, Characterisation of aquatic humic and non-humic matter with size-exclusion chromatography–organic carbon detection–organic nitrogen detection (LC-OCD-OND), *Water Res.* 45 (2011) 879–885.
- [65] N. Park, Y. Yoon, S.-H. Moon, J. Cho, Evaluation of the performance of tight-UF membranes with respect to NOM removal using effective MWCO, molecular weight, and apparent diffusivity of NOM, *Desalination* 164 (2004) 53–62.
- [66] E. Aoustin, A.I. Schäfer, A.G. Fane, T. Waite, Ultrafiltration of natural organic matter, *Sep. Purif. Technol.* 22 (2001) 63–78.
- [67] K. Dejaeger, J. Criquet, M. Vanoppen, C. Signal, G. Billon, E.R. Cornelissen, Identification of disinfection by-product precursors by natural organic matter fractionation: a review, *Environ. Chemistry Letters* 20 (2022) 3861–3882.
- [68] A.I. Schäfer, R. Mauch, T.D. Waite, A.G. Fane, Charge effects in the fractionation of natural organics using ultrafiltration, *Environ. Sci. Technol.* 36 (2002) 2572–2580.
- [69] T. Zhang, Z.-H. He, K.-P. Wang, X.-M. Wang, F.X. Yue-feng, L.a. Hou, Loose nanofiltration membranes for selective rejection of natural organic matter and mineral salts in drinking water treatment, *J. Membr. Sci.* 662 (2022) 120970.
- [70] J. Cho, G. Amy, J. Pellegrino, Membrane filtration of natural organic matter: factors and mechanisms affecting rejection and flux decline with charged ultrafiltration (UF) membrane, *J. Membr. Sci.* 164 (2000) 89–110.
- [71] S. Metsämuuronen, M. Sillanpää, A. Bhatnagar, M. Mänttari, Natural organic matter removal from drinking water by membrane technology, *Sep. Purif. Reviews* 43 (2014) 1–61.
- [72] D.S. Mallya, S. Abdikhebari, L.F. Dumée, S. Muthukumar, W. Lei, K. Baskaran, Removal of natural organic matter from surface water sources by nanofiltration and surface engineering membranes for fouling mitigation—A review, *Chemosphere* 138070 (2023).
- [73] A.I. Schäfer, A.G. Fane, T. Waite, Cost factors and chemical pretreatment effects in the membrane filtration of waters containing natural organic matter, *Water Res.* 35 (2001) 1509–1517.
- [74] W. Yu, T. Liu, J. Crawshaw, T. Liu, N. Graham, Ultrafiltration and nanofiltration membrane fouling by natural organic matter: Mechanisms and mitigation by pre-ozonation and pH, *Water Res.* 139 (2018) 353–362.
- [75] A. Imbrogno, A.I. Schäfer, Comparative study of nanofiltration membrane characterization devices of different dimension and configuration (cross flow and dead end), *J. Membr. Sci.* 585 (2019) 67–80.
- [76] L.-P. Cheng, H.-Y. Lin, L.-W. Chen, T.-H. Young, Solute rejection of dextran by EVAL membranes with asymmetric and particulate morphologies, *Polymer* 39 (1998) 2135–2142.
- [77] A. Jeihanipour, J. Shen, G. Abbt-Braun, S.A. Huber, G. Mkongo, A.I. Schäfer, Seasonal variation of organic matter characteristics and fluoride concentration in the Maji ya Chai River (Tanzania): Impact on treatability by nanofiltration/reverse osmosis, *Sci. Tot. Environ.* 637 (2018) 1209–1220.
- [78] A.I. Schäfer, Natural Organics Removal Using Membranes: Principles, Performance, and Cost, CRC Press, 2001.
- [79] E. Worch, Eine neue Gleichung zur Berechnung von Diffusionskoeffizienten gelöster Stoffe, *Vom Wasser* 81 (1993) 289–297.
- [80] Y.-A. Boussouga, T. Okkali, T. Luxbacher, A.I. Schäfer, Chromium (III) and chromium (VI) removal and organic matter interaction with nanofiltration, *Sci. Tot. Environ.* 885 (2023) 163695.
- [81] D.B. Burns, A.L. Zydney, Buffer effects on the zeta potential of ultrafiltration membranes, *J. Membr. Sci.* 172 (2000) 39–48.
- [82] A. Gopalakrishnan, M. Bouby, A.I. Schäfer, Membrane-organic solute interactions in asymmetric flow field flow fractionation: Interplay of hydrodynamic and electrostatic forces, *Sci. Tot. Environ.* 855 (2023) 158891.
- [83] J. Schaepe, C. Vandecasteele, B. Peeters, J. Luyten, C. Dotremont, D. Roels, Characteristics and retention properties of a mesoporous γ -Al₂O₃ membrane for nanofiltration, *J. Membr. Sci.* 163 (1999) 229–237.
- [84] Y.-A. Boussouga, H. Frey, A.I. Schäfer, Removal of arsenic (V) by nanofiltration: Impact of water salinity, pH and organic matter, *J. Membr. Sci.* 618 (2021) 118631.
- [85] G. Capannelli, I. Becchi, A. Bottino, P. Moretti, S. Munari, Computer driven porosimeter for ultrafiltration membranes, *Stud. Surf. Sci. Catal., Elsevier* (1988) 283–294.
- [86] J.I. Calvo, A. Bottino, G. Capannelli, A. Hernández, Comparison of liquid-liquid displacement porosimetry and scanning electron microscopy image analysis to characterise ultrafiltration track-etched membranes, *J. Membr. Sci.* 239 (2004) 189–197.
- [87] A. Ouattmane, M. Hafidi, M.E. Gharous, J. Revel, Complexation of calcium ions by humic and fulvic acids, *Analisis* 27 (1999) 428–431.
- [88] F.A. Johnson, D.Q. Craig, A.D. Mercer, Characterization of the block structure and molecular weight of sodium alginates, *J. Pharm. Pharmacol.* 49 (1997) 639–643.
- [89] C.-F. Lin, Y.-J. Huang, O.J. Hao, Ultrafiltration processes for removing humic substances: effect of molecular weight fractions and PAC treatment, *Water Res.* 33 (1999) 1252–1264.
- [90] I.V. Perminova, F.H. Frimmel, A.V. Kudryavtsev, N.A. Kulikova, G. Abbt-Braun, S. Hesse, V.S. Petrosyan, Molecular weight characteristics of humic substances from different environments as determined by size exclusion chromatography and their statistical evaluation, *Environ. Sci. Technol.* 37 (2003) 2477–2485.

- [91] R. Suwanpetch, J. Shiowatana, A. Siripinyanond, Using flow field-flow fractionation (FI-FFF) for observation of salinity effect on the size distribution of humic acid aggregates, *J. Environ. Anal. Chem.* 97 (2017) 217–229.
- [92] G. Yohannes, S.K. Wiedmer, M. Jussila, M.-L. Riekkola, Fractionation of humic substances by asymmetrical flow field-flow fractionation, *Chromatographia* 61 (2005) 359–364.
- [93] M.N. Nguyen, R. Hervas-Martínez, A.I. Schäfer, Organic matter interference with steroid hormone removal by single-walled carbon nanotubes– ultrafiltration composite membrane, *Water Res.* 199 (2021) 117148.
- [94] R.I. Peinador, J.I. Calvo, P. Prádanos, L. Palacio, A. Hernández, Characterisation of polymeric UF membranes by liquid–liquid displacement porosimetry, *J. Membr. Sci.* 348 (2010) 238–244.
- [95] S.T. Akhil Gopalakrishnan, Youssef-Amine Bousouga, Andrea I. Schäfer, Nanofiltration membranes in asymmetric flow field-flow fractionation for improved organic matter size fractionation, Unpublished work, (2023).
- [96] I.I. Ryzhkov, A.V. Minakov, Theoretical study of electrolyte transport in nanofiltration membranes with constant surface potential/charge density, *J. Membr. Sci.* 520 (2016) 515–528.